Cell Cycle 13:1, 126–137; January 1, 2014; © 2014 Landes Bioscience

Inhibition of endocytic vesicle fusion by Plk1-mediated phosphorylation of vimentin during mitosis

Keisuke Ikawa[1,2], Ayaka Satou[3], Mitsuko Fukuhara[1,2], Shigeru Matsumura[1,2], Naoyuki Sugiyama[3], Hidemasa Goto[4], Mitsunori Fukuda[5], Masaki Inagaki[4], Yasushi Ishihama[3,*], and Fumiko Toyoshima[1,2,*]

[1]Department of Cell Biology; Institute for Virus Research; Kyoto University; Sakyo-ku, Kyoto, Japan; [2]Department of Mammalian Regulatory Network; Graduate School of Biostudies; Kyoto University; Sakyo-ku, Kyoto, Japan; [3]Department of Molecular & Cellular BioAnalysis; Graduate School of Pharmaceutical Sciences; Kyoto University; Sakyo-ku, Kyoto, Japan; [4]Division of Biochemistry; Aichi Cancer Center Research Institute; Chikusa-ku, Nagoya, Japan; [5]Department of Developmental Biology and Neurosciences; Graduate School of Life Sciences; Tohoku University; Sendai, Miyagi, Japan

Keywords: endosome, mitosis, Plk1, vesicle fusion, vimentin

Endocytic vesicle fusion is inhibited during mitosis, but the molecular pathways that mediate the inhibition remain unclear. Here we uncovered an essential role of Polo-like kinase 1 (Plk1) in this mechanism. Phosphoproteomic analysis revealed that Plk1 phosphorylates the intermediate filament protein vimentin on Ser459, which is dispensable for its filament formation but is necessary for the inhibition of endocytic vesicle fusion in mitosis. Furthermore, this mechanism is required for integrin trafficking toward the cleavage furrow during cytokinesis. Our results thus identify a novel mechanism for fusion inhibition in mitosis and implicate its role in vesicle trafficking after anaphase onset.

Introduction

The endocytic system plays a central role in sorting and distributing internalized cargoes within the endocytic vesicles.[1,2] The internalized cargoes are carried into early endosomes and then recycled back to the plasma membrane or transferred to the late endosome–lysosome pathway to be degraded.[1,2] During interphase, early endosomes constitutively undergo heterotypic and homotypic fusion with incoming vesicles, which constitutes the endocytic system. In mitosis the fusion of the endocytic vesicles is transiently inhibited,[3] and this fusion inhibition is rescinded at the onset of telophase, at which time endosomal vesicles travel toward the midbody to insert membrane at the cytokinesis furrow.[4-7] The regulatory mechanisms for the inhibition of endocytic vesicle fusion in mitosis are largely unknown. It is known, nonetheless, that endocytic vesicle fusion depends on the activity of a small GTPase Rab5 and its effector protein, early endosomal antigen 1 (EEA1).[1,2,8] EEA1 also associates with phosphatidylinositol-3-phosphate (PtdIns3P) through the C-terminal FYVE domain, which enhances the recruitment of EEA1 to early endosomes.[1,2,9] An early paper using a cell-free fusion assay with *Xenopus* mitotic extracts found a requirement for cyclin-dependent kinase 1 (Cdk1) in the fusion inhibition in mitosis.[3] In addition, RN-tre, a GTPase-activating protein for Rab5, is phosphorylated by Cdk1 in vitro, and this phosphorylation increases the GAP activity of RN-tre toward Rab5 in mitosis.[10] It has also been reported that the class III phosphoinositide kinase Vps34, which produces PtdIns3P on early endosomes,[1,2,11] is phosphorylated by Cdk1 in mitosis, and this phosphorylation negatively regulates its kinase activity by blocking the interaction between Vps34 and its regulatory protein Beclin.[12] Therefore, Cdk1 appears to be a central regulator for fusion inhibition in mitosis. However, direct evidence for the requirement of RN-tre, Rab5, and Vps34 for fusion inhibition during mitosis is lacking. Moreover, the involvement of other mitotic regulators in this mechanism has not been investigated.

In this study, we have found that Polo-like kinase (Plk) 1, a serine–threonine kinase that regulates multiple aspects of mitosis, including centrosome maturation, spindle assembly, Golgi fragmentation, and cytokinesis,[13-17] plays an essential role in the inhibition of vesicle fusion during mitosis. We have identified a substrate of Plk1 in this mechanism and propose its role in vesicle trafficking after anaphase onset.

Results

To gain insight into the function of Plk1 in endosome dynamics during mitosis, we first measured the volume of early endosomes in HeLa cells synchronized in M phase. We found that depletion of Plk1 by either of 2 different siRNAs induced the enlargement of early endosomes, which were quantified by measuring the volume of EEA1-positive vesicles (**Fig. 1A–C**). The

*Correspondence to: Fumiko Toyoshima; Email: ftoyoshi@virus.kyoto-u.ac.jp; Yasushi Ishihama; Email: yishiham@pharm.kyoto-u.ac.jp
Submitted: 08/02/2013; Revised: 10/18/2013; Accepted: 10/18/2013
http://dx.doi.org/10.4161/cc.26866

expression level of EEA1 protein was not changed by the Plk1 depletion (**Fig. S1A**), excluding the possibility that the enlargement of EEA1-positive vesicles resulted from the increase in the expression level of EEA1 proteins. The Plk1 depletion-induced enlargement of early endosomes in M-phase cells was rescued by the expression of GFP-tagged mouse Plk1, which is resistant to the human Plk1 siRNA (**Fig. 1D and E**). In addition, treatment of the cells with the Plk1 kinase inhibitor BI2536 induced a similar phenotype in M-phase cells (**Fig. S1B**). Importantly, BI2536 treatment or Plk1 depletion did not induce the enlargement of early endosomes in S phase-arrested cells (**Fig. S1C**), nor did it induce the enlargement of late endosomes in M-phase cells, which were quantified by measuring the volume of CIMPR-positive vesicles (**Fig.S1D and E**). These results suggest that Plk1 regulates early endosome dynamics during mitosis.

A previous study reported that fusion of endocytic vesicles results in the enlargement of early endosomes.[18] We therefore hypothesized that depletion of Plk1 might cause abnormal endocytic vesicle fusion in mitosis, which would explain the enlargement of early endosomes. To analyze the fusion of endocytic vesicles in cells, cells arrested in M phase or in S phase (interphase) were incubated with Alexa647-labeled EGF for 5 min to internalize the labeled EGF, washed with acid buffer, followed by incubation with Alexa555-labeled EGF for 5 min, washed with culture medium, and then incubated for an additional 5 min to allow for the fusion of endocytic vesicles (**Fig. 1F**). In control experiments, we confirmed that the internalized labeled EGF resided within the early endosomes, but it was not closely associated with the endosomal membrane in interphase cells that ectopically expressed an active form of Rab5A (Rab5CA), which localized on the endosomal membrane (**Fig. S2A**). Therefore, if the endocytic vesicles were to undergo endosome fusion, the volume of the vesicles with merged signals of Alexa647 and Alexa555 would increase. To define the endocytic vesicles that underwent endosome fusion, we measured the volume of each vesicle that displayed merged signals of Alexa647 and Alexa555. In interphase cells, the volume of the vesicles with merged signals was larger than 200 voxel in more than 25% vesicles in the control cells, whereas the volumes of all vesicles in the cells depleted with NSF and α-SNAP, the essential regulators for endosome fusion,[19,20] fell within 200 voxel (**Fig. S2B and C**). Thus, we judged a vesicle with merged signals as an endocytic vesicle that underwent endosome fusion when the volume of the merged signals was larger than 200 voxel.

Using this system, we analyzed endocytic vesicle fusion in M-phase cells. We often observed large vesicles with merged signals in the Plk1-depleted cells when compared with that in control cells (**Fig. 1G** upper; histogram). The frequency of endosomal fusion was significantly increased in the Plk1-depleted cells when compared with that in control cells (**Fig. 1G**, bottom inset). It should be noted that in control M-phase cells, the vesicles with Alexa647-EGF were often adhered to the vesicles with Alexa555-EGF (**Fig. 1G**, upper left) as in the interphase cells depleted with NSF and α-SNAP (**Fig. S2C**), suggesting that endosome docking seems to occur during mitosis. Depletion of Plk1 did not alter the frequency of endosome docking, which can be quantified by the ratio (%) of vesicles with merged signals to the number of Alexa555-positive vesicles (**Fig. 1H**). Time-lapse images of the M phase-arrested cells which were incubated sequentially with Alexa488-EGF and Alexa555-EGF showed that the endocytic vesicles were attached to each other but rarely underwent vesicle fusion in control cells, but abnormally fused to each other in the Plk1-depleted cells (**Fig. 1I**; **Videos S1 and 2**). These results demonstrate that inhibition of endocytic vesicle fusion during mitosis is mediated by Plk1.

In order to identify Plk1 substrates that are involved in the inhibition of endocytic vesicle fusion in mitosis, we purified the early endosome fraction from M phase-arrested HeLa cells by sucrose gradient centrifugation (**Fig. 2A**). First, to confirm that Plk1 target proteins were indeed present in the early endosome fraction, we performed an in vitro kinase assay using purified recombinant Plk1 proteins and [γ-^{32}P] ATP. We detected radiolabeled proteins that were phosphorylated by recombinant wild-type (WT) Plk1, but not by kinase-dead (KD) Plk1 (**Fig. 2B**). Then, to identify the Plk1 substrates, the early endosome fraction was dephosphorylated, incubated with WT-Plk1 or KD-Plk1, and then digested with trypsin. The tryptic digests from WT-Plk1 or KD-Plk1 treatment were labeled with $^{13}CD_2O$ (heavy label) or CH_2O (light label), respectively,[21,22] and were mixed. After desalting, the labeled peptides were subjected to a titanium dioxide (TiO2)-based phosphopeptide enrichment, followed by nano-scale liquid chromatography-tandem mass spectrometry (nanoLC-MS/MS). We identified 40 heavy-labeled phosphopeptides whose peak area was more than twice the size of the light-labeled ones (**TableS1**). Among them, Ser459 of vimentin has been previously reported to be phosphorylated in mitotic cells.[23] In addition, this residue is conserved in several vertebrate species (**Fig. 2C**). The MS signal for the phosphopeptide, including Ser459 of vimentin, was easily detected in the sample that had been incubated with WT-Plk1 but hardly detected in the sample with KD-Plk1 (**Fig. 2D**; **Fig. S3A**). In addition, recombinant WT-Plk1, but not KD-Plk1, efficiently phosphorylated purified vimentin (**Fig. 2E**) on Ser 459 in an in vitro kinase assay (**Fig. 2F**; **Fig. S3B**). Furthermore, quantitative nanoLC-MS/MS analysis of the vimentin-derived phosphopeptide (pS459) revealed that the vimentin phosphorylation on Ser 459 was significantly upregulated in the M-phase arrested cells, compared with the BI2536-treated, M phase-arrested cells (**Fig. 2G**; **Fig. S3C**) or the G/S phase-arrested cells (**Fig. 2H**; **Fig. S3C**). These results demonstrate that Plk1 directly phosphorylates vimentin on Ser 459 during mitosis.

Next, we examined whether the phosphorylation of vimentin on Ser459 is required for the inhibition of endocytic vesicle fusion in mitosis. Depletion of vimentin by RNAi induced the enlargement of early endosomes in M-phase cells (**Fig. 3A and B**), but not in S phase cells (**Fig. S4A and B**). In addition, the frequency of endocytic vesicle fusion was significantly increased in the vimentin-depleted cells, when compared with that in control cells (**Fig. 3C and D**; Luci si+GFP vs. Vim si+GFP). Introduction of GFP-tagged WT-mouse vimentin, which is resistant to the human vimentin siRNA, or GFP-tagged S459E-mouse vimentin, a phosphomimic mutated form of vimentin in which Ser459 was

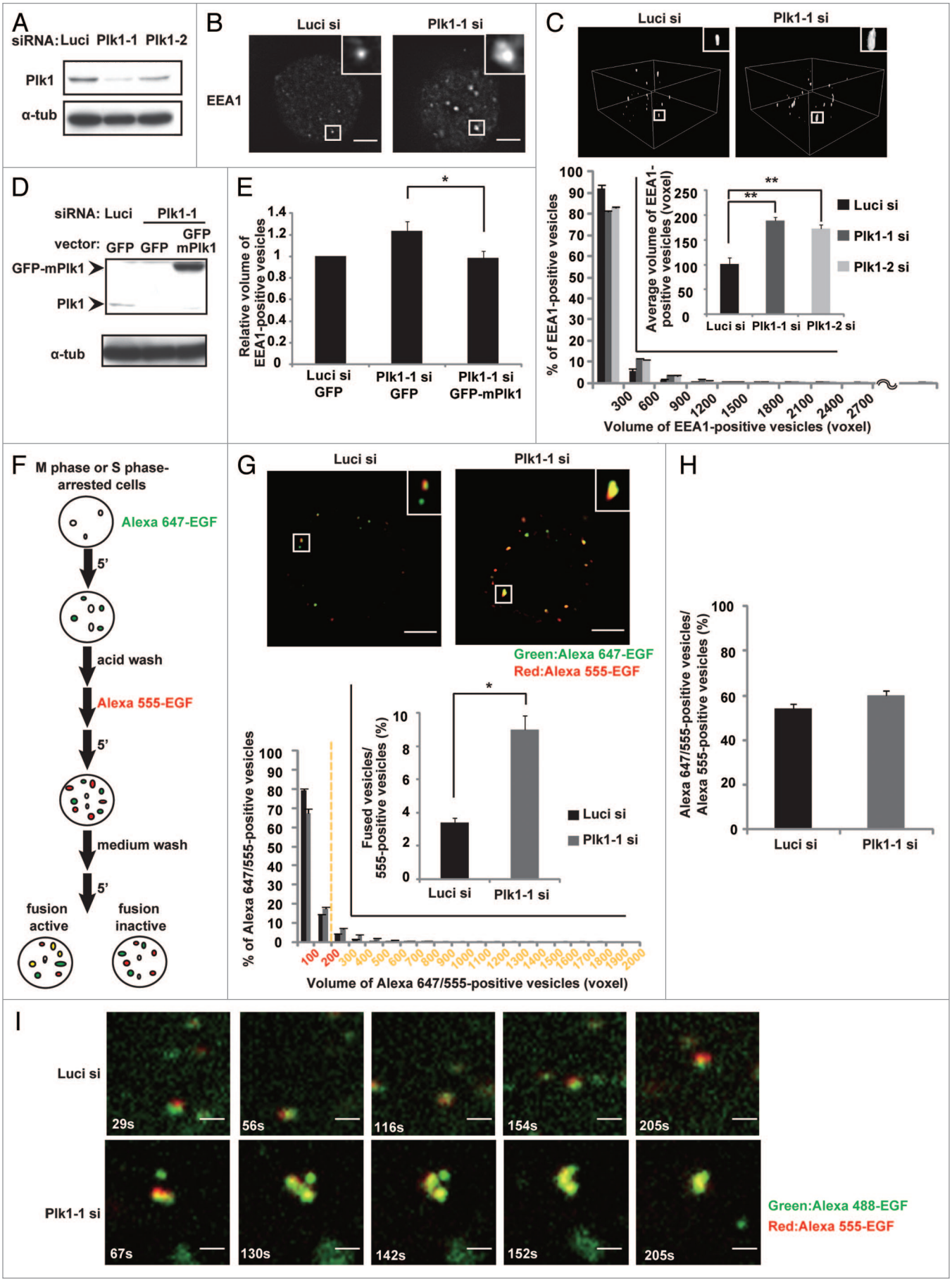

Figure 1 (See opposite page). Plk1 is required for the inhibition of endocytic vesicle fusion in mitosis. (**A**) Western blot analysis for the expression of Plk1 and control α-tubulin in M-phase synchronized cells transfected with the indicated siRNAs. (**B**) Images of EEA1 in M-phase cells treated as in (**A**). (**C**) 3D construction images of EEA1 in the cells in (**B**) (upper). Distribution (histogram; n = 30) and the average (inset; mean ± s.e.m. from 3 different experiments; n = 30/experiment) of the volumes of the EEA1-positive vesicles are shown in the lower part of the panel. $^{**}P < 0.01$, analyzed by Dunnett multiple-comparison test. One voxel represents 0.00027 μm^3. (**D**) Western blot analysis of Plk1, GFP-mouse Plk1, and α-tubulin from M-phase synchronized cells transfected with the indicated siRNAs together with the indicated plasmids. (**E**) The relative volume of the EEA1-positive vesicles in the cells treated as in (**D**). $^{*}P < 0.05$, analyzed by *t* test. (**F**) Flow diagram of the in-cell fusion assay. (**G**) The in-cell fusion assay in M-phase cells. M phase-arrested cells transfected with the indicated siRNAs were incubated sequentially with Alexa 647-EGF and Alexa 555-EGF as described in (**F**). The merged images of Alexa 647-EGF and Alexa 555-EGF are shown (upper). Distribution of the volume of the Alexa 647- and Alexa 555-positive vesicles is shown in the histogram (n = 30). A vesicle with a volume of more than 200 voxels is defined as a fused vesicle (yellow). The inset graph shows the average population of the Alexa 555-positive vesicles that are defined as fused vesicles. (mean ± s.e.m. from 3 different experiments; n = 30/experiment). $^{**}P < 0.01$, analyzed by *t* test. The scale bar represents 5 μm. (**H**) The average population of the Alexa 555-positive vesicles that are defined as docking or fused vesicles in the cells in (**F**) (mean ± s.e.m. from 3 different experiments; n = 30/experiment). (**I**) Time-lapse images of metaphase cells transfected with the indicated siRNAs and incubated sequentially with Alexa 555-EGF and Alexa 488-EGF as in (**F**). The scale bar represents 1 μm.

replaced by Glu, suppressed the abnormal vesicle fusion during M phase in the vimentin-depleted cells (**Fig. 3C–F**), but GFP-tagged S459A-mouse vimentin, a non-phosphorylatable form of vimentin in which Ser459 was replaced by Ala, did not (**Fig. 3C and D**). Importantly, the Plk1 depletion-induced abnormal vesicle fusion during M phase was significantly suppressed by the introduction of GFP-tagged S459E-mouse vimentin in the vimentin-depleted cells, but not by GFP-tagged S459A-mouse vimentin (**Fig. 3G and H**), indicating that the abnormal vesicle fusion caused by the Plk1 depletion depends on the failure of vimentin phosophorylation on Ser459. Like the Plk1 depletion, vimentin depletion did not alter the frequency of endosome docking in the presence or absence of GFP-tagged WT, S459A, or S459E mouse vimentin (**Fig. S4C–E**). These results demonstrate that Plk1-mediated phosphorylation of vimentin on Ser459 is required for the inhibition of endocytic vesicle fusion in mitosis. It was previously shown that Plk1 phosphorylates vimentin on Ser82,[16,24] and this phosphorylation promotes vimentin filament segregation.[16] However, ectopically expressed GFP-tagged S459A-mouse vimentin could still form filament structures in vimentin-depleted interphase cells similarly to GFP-tagged WT-mouse vimentin (**Fig. S4F**). Therefore, phosphorylation of vimentin on Ser459 promotes the inhibition of the endocytic vesicle fusion during mitosis without altering the polymerization or filament formation activity of vimentin proteins.

Then, what will happen to the cargos, if the endocytic vesicles are abnormally fused to each other during mitosis? To address this issue, we examined integrin trafficking during cell division. Interestingly, we found that, during metaphase, β1-integrin vesicles were associated with both GFP-Rab5A and GFP-Rab21 in control cells, but merely associated with GFP-Rab21 in the vimentin-depleted cells (**Fig. 4A and B**) or in cells treated with BI2536 (**Fig. S5A**), although the association of GFP-Rab5A to the β1-integrin vesicles was still observed in these cells (**Fig. 4A**). It has been recently reported that integrins are transported to the cleavage furrow through Rab21-dependent vesicle trafficking.[5] We therefore investigated the role of Plk1-mediated phosphorylation of vimentin Ser459 in integrin trafficking during ana/telophase. Time-lapse images of cells incubated with Alexa546-labeled–anti-β1-integrin antibodies, and following the endocytosis of the labeled antibodies, showed that internalized antibodies accumulated at the cleavage furrow during anaphase and became concentrated at the ingressing cleavage furrow during telophase in control cells, as reported previously,[5] whereas they hardly accumulated at the cleavage furrow during ana/telophase in the vimentin-depleted cells (**Fig. 4C**). The intensity of β1-integrin signals at the cleavage furrow in telophase cells was significantly reduced in the vimentin-depleted cells when compared with that in control cells (**Fig. 4D and E**; **Fig. S5B**). The reduction of β1-integrin signals at the cleavage furrow in the vimentin-depleted cells was rescued by expression of GFP-tagged WT-mouse vimentin, but not by GFP-tagged S459A-mouse vimentin in these cells (**Fig. 4D and E**; **Fig. S5B**). β1-integrins accumulated at the cleavage furrow in more than 70% of the control telophase cells, but in less than 20% of the vimentin-depleted telophase cells (**Fig. 4F**). Expression of GFP-tagged WT-mouse vimentin, but not GFP-tagged S459A-mouse vimentin, again restored the accumulation of β1-integrins at the cleavage furrow in the vimentin-depleted telophase cells (**Fig. 4F**). The previous report has shown that the failure in β1-integrin trafficking toward the cleavage furrow causes defects in cytokinesis.[5] Consistent with the report and our results showing the defects in β1-integrin trafficking toward the cleavage furrow in the vimentin-depleted cells (**Fig. 4C–F**), the population of multinucleated cells was increased in the vimentin-depleted cells when compared with that in control cells (**Fig. 4G**). Expression of GFP-tagged WT-mouse vimentin or GFP-tagged S459E-mouse vimentin, but not GFP-tagged S459A-mouse vimentin, suppressed the appearance of multinucleated cells in the vimentin-depleted cells (**Fig. 4G**). Therefore, Plk1-mediated phosphorylation of vimentin on Ser459 is required for β1-integrin trafficking toward the cleavage furrow to promote successful cytokinesis. We infer that inhibition of endocytic vesicle fusion by the Plk1-vimentin pathway may be a prerequisite for loading Rab21 to the integrin vesicles during metaphase, which ensures the integrin trafficking toward the cleavage furrow after anaphase onset.

Discussion

This study identified the Plk1–vimentin pathway for a novel mechanism for the inhibition of endocytic vesicle fusion in mitosis. Endocytic vesicle fusion requires the activity of Rab5 and its target EEA1.[1,2,8,9] Thus, Plk1 might inhibit Rab5-EEA1 pathway during mitosis. However, GFP-Rab5A signals were detected on the endocytic β1-integrin vesicles in both control cells and vimentin-depleted cells (**Fig. 4A**). In addition, Plk1-depletion did

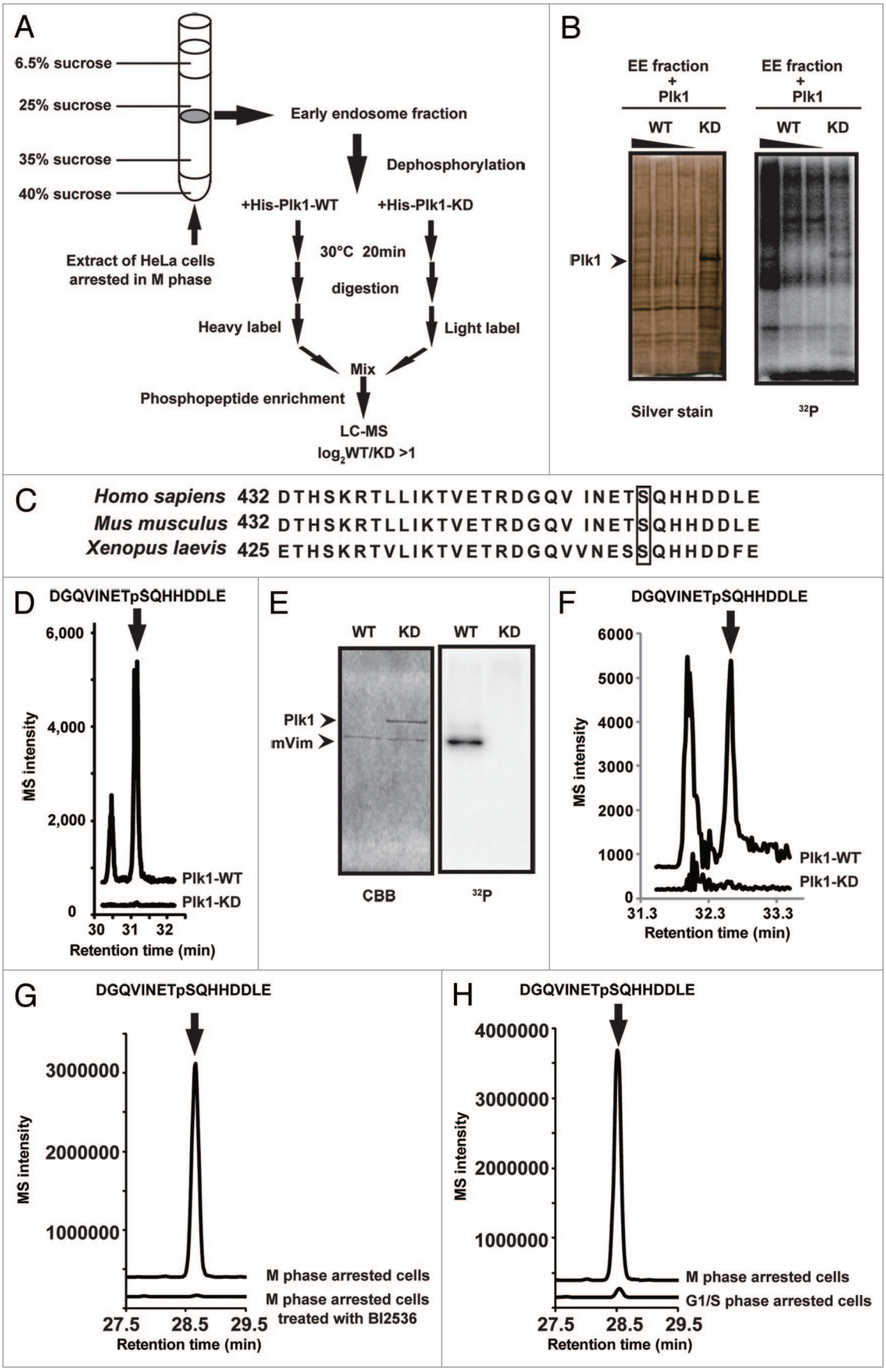

Figure 2. For figure legend, see page 131.

not alter the activity of Rab5, which can be monitored by GST-pull down assay using GST-conjugated Rab5 binding domain of Rabaptin5 proteins, in M phase-synchronized cells (**Fig. S6A**). Moreover, the signal of the FYVE domain of EEA1, which monitors PtdIns3P on early endosomes, was hardly detected on the early endosomes in the control cells as well as in the cells treated with the Plk1 inhibitor BI2536 during M phase (**Fig. S6B**, left), whereas in interphase cells it could be detected on the early endosomes in the control cells but not in the cells treated with a Vps34 inhibitor wortmannin (**Fig.S6B**, right). Thus, it seems unlikely that the Plk1–vimentin module inhibits vesicle fusion by suppressing the activation of Rab5 or Vps34. Interestingly, however, we have found that GFP-tagged WT-mouse vimentin proteins reside in the early endosome fractions purified from the M phase-arrested cells, as described in the previous report using asynchronized cells[25] (**Fig. S4G**, left). Although our results using GFP-tagged S459A-mouse vimentin show that Ser 459-phosphorylation is not required for targeting of vimentin to the early endosome fractions (**Fig. S4G**, right), it is possible that vimentin associates with and recruits a protein(s), which is required for the inhibition of endocytic vesicle fusion during mitosis, to the early eondosomes in a Ser459 phosphorylation-dependent manner. Recent report has demonstrated that the binding kinetics of EEA1 to the endosomal membrane can be separated into 2 fractions: one rapidly exchanging with cytosolic pool, and the other is the immobile fraction. [26] Interestingly, it has been shown that during mitosis, the dissociation rate of EEA1 from early endosomes is accelerated, and the immobile fraction is reduced.[26] The Ser 459-phsophrylated form of vimentin may associate with a protein(s) that alters the binding kinetics of EEA1 to the early endosomes during mitosis. Identification of the proteins that interact with the Ser459-phosphorylated form of vimentin in mitotic cells should be clarified in future studies.

Fusion inhibition is thought to be involved in organelle fragmentation during mitosis.[3,27,28] In this study, we raises a possible role of the mitotic fusion inhibition for the spatial control of endosome trafficking after anaphase onset. We speculate that fusion inhibition may keep the individual cargo resides in a separated endosome, which ensures the loading of Rab proteins specific for each cargo to the endosome, in order to promote the rapid targeting of cargos in the endocytic vesicles to pre-determined positions immediately after the end of mitosis. Considering an emerging role of endosome trafficking during cytokinesis for the signal transduction in asymmetric cell division,[27,28] inhibition of endocytic vesicle fusion might be generally required for the directional endosome trafficking during cell division.

Materials and Methods

Cell culture and antibodies

HeLa cells were cultured in Dulbecco modified Eagle medium with 10% fetal bovine serum (DMEM). Cells were cultured on native collagen and synchronized by a double-thymidine block. BI2536 (Axon Medchem) was dissolved in DMSO (5mM) and stored at –20 °C. The antibodies used included anti-Plk1 (Invitrogen), anti-EEA1 (BD Transduction Laboratories), anti-CIMPR (Thermo Scientific), anti-α-tubulin (Sigma), anti-α-SNAP (Abcam), anti-NSF (Calbiochem), anti-vimentin (Santa Cruz), and anti-β1-integrin (P5D2, Abcam).

In-cell vesicle fusion assay

HeLa cells were arrested in metaphase or in S phase by treatment with MG132 (Wako) or thymidine, respectively. Cells were then incubated with Alexa647-EGF (Invitrogen) at 37 °C for 5 min, washed with acid wash buffer (200 mM NaCl, 50 mM MES, pH 5.0) at 4 °C for 5 min, incubated with Alexa555-EGF (Invitrogen) for 5 min, washed with DMEM, and then further incubated at 37 °C for 5 min. Cells were fixed with 3.7% formalin for 10 min at 37 °C. Z stack images (0.3 μm apart) of the metaphase cells were obtained and processed by 3D deconvolution using Meta Morph software (Moleculer Devices). The Z stack images of Alexa647-EGF and Alexa555-EGF were merged, and the particles with merged signals were defined by ImageJ. The voxels of the particles with merged signals were measured using Meta Morph software. For live cell imaging, HeLa cells were arrested in metaphase, sequentially incubated with Alexa555-EGF and Alexa488-EGF as described above, and washed with DMEM. Time-lapse images were obtained with a CV1000 confocal microscope (YOKOGAWA) at 37 °C with 5% CO_2. The images were recorded at 1 s intervals for 15 min.

siRNA experiments

For depletion of human Plk1 and vimentin, siRNAs were designed to target the following sequences: Plk1-1, 5′-ggttttcgat tgctcccag-3′; Plk1-2, 5′-gggcggcttt gccaagtgc-3′; vimentin, 5′-gggaaactaa tctggattc-3′. These oligonucleotides were purchased from Japan Bioservice. The siRNAs targeting human α-SNAP and NSF were purchased from Dharmacon (siGENOMESMARTpool). HeLa cells were transfected with siRNA by using Oligofectamine (Invitrogen), incubated for 4 h and synchronized by a double-thymidine block. The expression levels of the proteins were analyzed by immunoblotting.

Plasmid constructs and transfection

GFP-mouse Plk1 was described previously.[17] GFP-mouse Rab5A, GFP-mouse Rab5CA and GFP-mouse Rab21 were

Figure 2 (See opposite page). Plk1 phosphorylates vimentin on Ser459. (**A**) Flow diagram of the phosphoproteome analysis to identify Plk1 substrates in the early endosome fractions. (**B**) The in vitro kinase assay of His-tagged WT-Plk1 (0.05, 0.01, 0.005 μg) and His-tagged KD-Plk1 (0.3 μg) with early endosome fractions. The silver-stained SDS-PAGE gel (left) and corresponding autoradiogram (^{32}P) (right) are shown. (**C**) Sequence alignment of the vimentin C-terminus from 3 vertebrate species, showing a conserved serine residue (Ser459 in human). (**D**) The results of phosphoproteome analysis of the early endosome fraction. The ion current chromatogram of DGQVINETpSQHHDDLE extracted from the annotated MS/MS spectrum (**Fig. S3A**) is shown. (**E**) The in vitro kinase assay of His-tagged WT-Plk1 (0.05 μg) or His-tagged KD-Plk1 (0.3μg) and recombinant vimentin substrate (1.5 μg). Gel images after Coomassie brilliant blue (CBB) staining (left) and autoradiography (^{32}P) (right) are shown. (**F**) The ion current chromatogram of DGQVINETpSQHHDDLE extracted from the annotated MS/MS spectrum (**Fig. S3B**) in the Plk1-vimentin reaction. (**G**) The results of phosphoproteome analysis of the M phase-arrested cells treated with or without BI 2536. The ion current chromatogram of DGQVINETpSQHHDDLEextracted from the annotated MS/MS spectrum (**Fig. S3C**) is shown. (**H**) The results of phosphoproteome analysis of the cells arrested in M phase or G_1/S phase. The ion current chromatogram of DGQVINETpSQHHDDLE extracted from the annotated MS/MS spectrum (**Fig. S3C**) is shown.

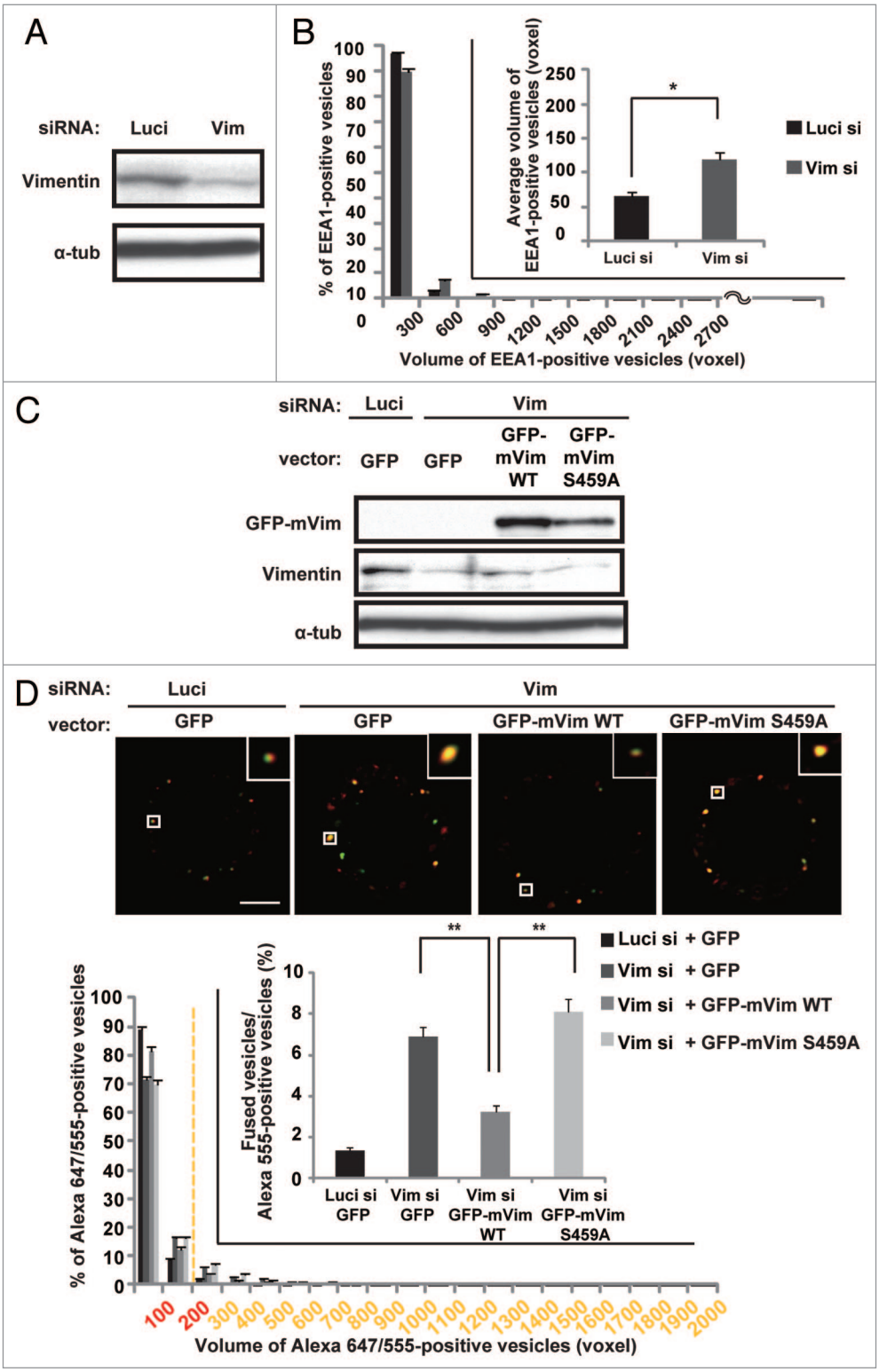

Figure 3A–D. Phosphorylation of vimentin on Ser459 is required for the inhibition of endocytic vesicle fusion in mitosis. (**A**) Western blot analysis of vimentin and control α-tubulin in M-phase synchronized cells transfected with the indicated siRNAs. (**B**) Distribution (histogram; mean ± s.e.m. from 3 different experiments; n = 30/experiment) and the average (inset; mean ± s.e.m. from 3 different experiments; n = 30/experiment) volume of the EEA1-positive vesicles in cells treated as in (**A**). **P* < 0.05, analyzed by *t* test. (**C**) Western blot analysis of vimentin, GFP-mouse WT- or S459A-vimentin, and α-tubulin in M-phase synchronized cells transfected with the indicated siRNAs together with the indicated plasmids. (**D**) The in-cell fusion assay of the cells in (**C**). The merged images of Alexa 647-EGF and Alexa 555-EGF in metaphase-arrested cells are shown (upper). Distribution of the volume of the Alexa 647/555-positive vesicles is shown in the histogram (mean ± s.e.m. from 3 different experiments; n = 30/experiment). The inset graph shows the average population of the Alexa 555-positive vesicles that are defined as fused vesicles (mean ± s.e.m. from 3 different experiments; n = 30/experiment). ***P* < 0.01, analyzed by Dunnett multiple-comparison test. The scale bar represents 5 μm.

described previously.[29,30] Mouse vimentin cDNA was subcloned into pEGFP-N (Clontech). GFP-mouse S459A- and S459E-vimentin were generated using a QuickChange Site-Directed Mutagenesis Kit (Stratagene). HeLa cells were transfected with plasmids by using Lipofectamine Plus (Invitrogen) after the first release of a double-thymidine block, incubated for 30 min and washed with fresh medium.

Early endosome fractionation

We modified a method that was previously described.[8] Briefly, HeLa cells were cultured in 100-mm dishes and synchronized by a double-thymidine block. Ten hours after release from the double-thymidine block, the cells were treated with MG132 (Wako) for 2 h to arrest them in mitosis and collected in 15 ml tubes. After washing with homogenization buffer (25 mM sucrose, 3 mM imidazole, pH 7.4), the cells were suspended in 1.5 ml homogenization buffer containing protease inhibitors (10 μg/ml aprotinin, 1 μg/ml pepstatin, 1 μg/ml antipain) and 0.5 mM EDTA. Cells were then homogenized and centrifuged for 10 min at 3000 rpm at 4 °C. The collected postnuclear supernatants were adjusted to 40% sucrose, loaded at the bottom of a step gradient consisting of 3 successive cushions of 35%, 25%, and 6.5% sucrose in 3 mM imidazole, pH 7.4, and then centrifuged at 32 000 rpm for 90 min at 4 °C. The early endosome fraction was collected from the interface between the 35% and 25% sucrose layers. For fractionation of the early endosomes and late endosomes in **Fig. S4G**, samples (500 ml per fraction) were collected from the top of the sucrose cushions and subjected to western blot analysis.

Protein preparation and kinase assay

Recombinant His-tagged human Plk1-WT was purchased from Sigma. Recombinant His-tagged mouse Plk1-KD was expressed in *Escherichia coli* and purified by affinity

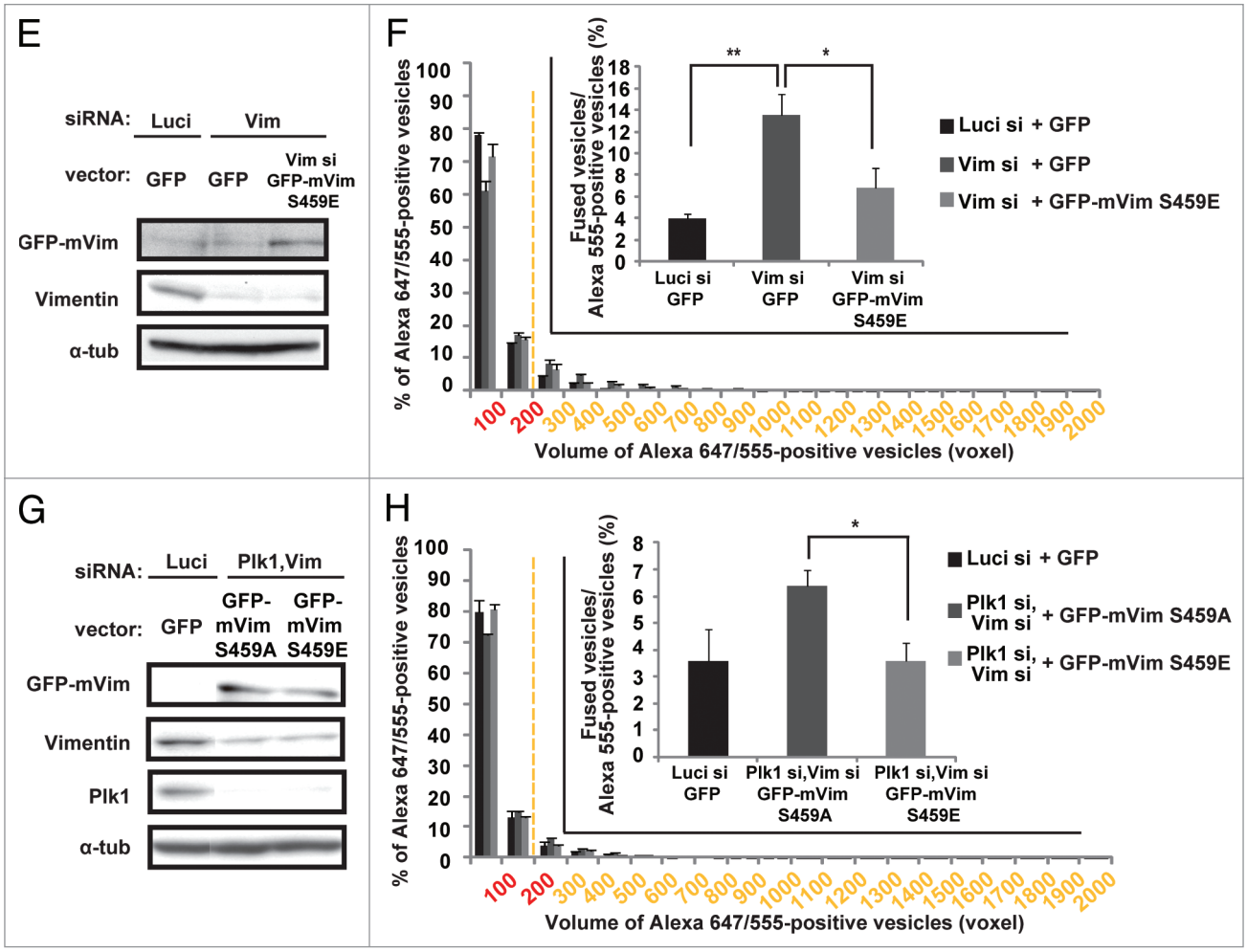

Figure 3E–H. (**E**) Western blot analysis of vimentin, GFP-mouse S459E-vimentin, and α-tubulin in M-phase synchronized cells transfected with the indicated siRNAs together with the indicated plasmids. (**F**) The in-cell fusion assay of the cells in (**E**). Distribution of the volume of the Alexa 647/555-positive vesicles is shown in the histogram (mean ± s.e.m. from 3 different experiments; n = 30/experiment). The inset graph shows the average population of the Alexa 555-positive vesicles that are defined as fused vesicles (mean ± s.e.m. from 3 different experiments; n = 30/experiment). *$P < 0.05$, **$P < 0.01$, analyzed by Dunnett multiple-comparison test. (**G**) Western blot analysis of vimentin, Plk1, GFP-mouse S459A-, or S459E-vimentin, and α-tubulin in M-phase synchronized cells transfected with the indicated siRNAs together with the indicated plasmids. (**H**) The in-cell fusion assay of the cells in (**E**). Distribution of the volume of the Alexa 647/555-positive vesicles is shown in the histogram (mean ± s.e.m. from 3 different experiments; n = 30/experiment). The inset graph shows the average population of the Alexa 555-positive vesicles that are defined as fused vesicles. (mean ± s.e.m. from 3 different experiments; n = 30/experiment). *$P < 0.05$, analyzed by *t* test.

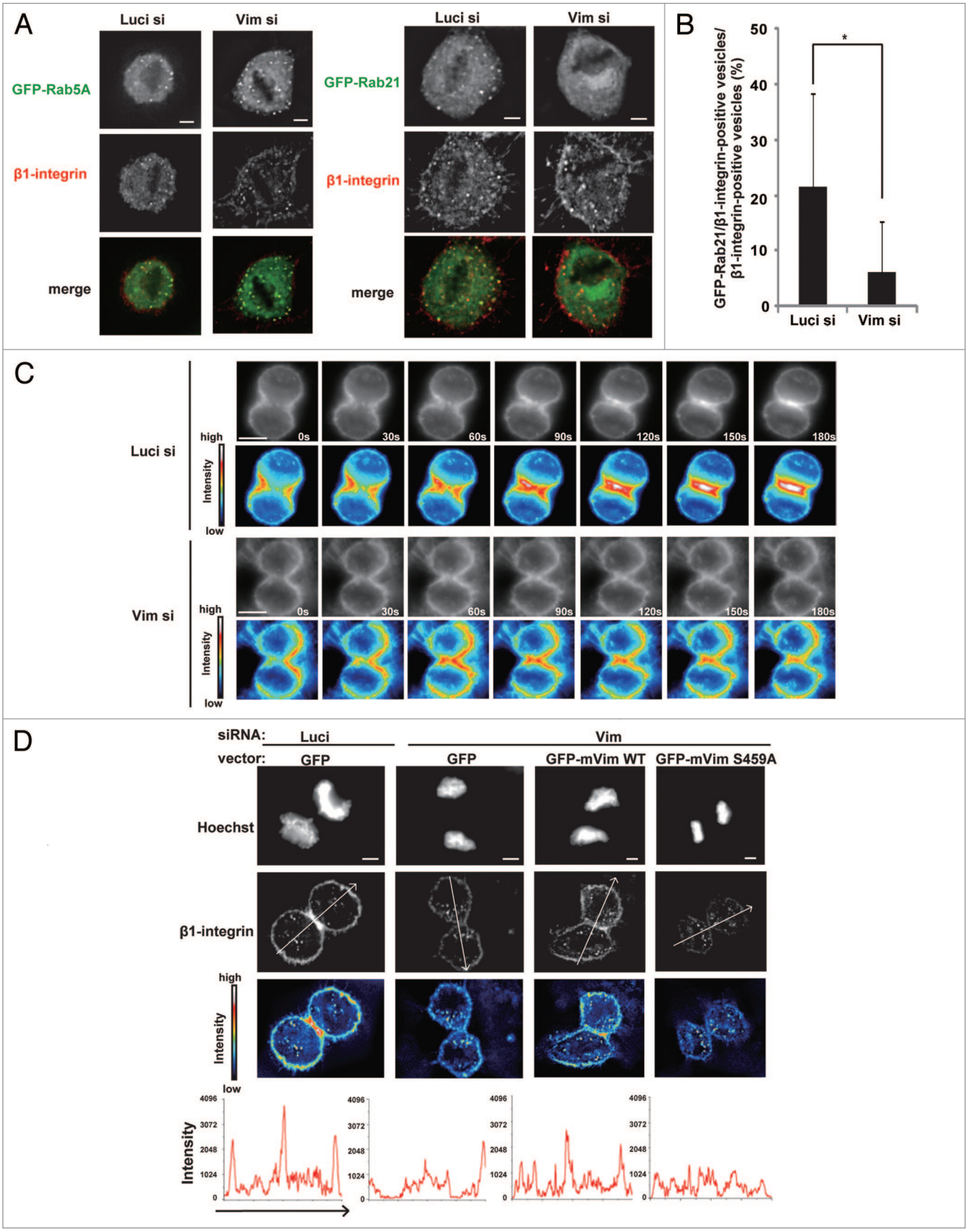

Figure 4A–F. For figure legend, see page 135.

Figure 4A–D (See opposite page). Phosphorylation of vimentin on Ser459 is required for integrin trafficking toward the cleavage furrow. (**A**) Images of metaphase cells transfected with the indicated siRNAs together with GFP-Rab5A (left) or GFP-Rab21 (right), incubated with Zenon-Alexa 546-labeled anti-β1-integrin antibodies for 30 min to allow for endocytosis of the labeled antibody, washed with medium, and incubated for an additional 30 min. (**B**) The average percentage of the population of β1-integrin-positive vesicles that associate with Rab21 in the cells in (**A**). (**C**) Time-lapse images of the dividing cells transfected with the indicated siRNAs and treated with the labeled anti-β1-integrin antibody as in (**A**). Heat map images are shown underneath. (**D**) Images of telophase cells transfected with the indicated siRNAs together with the indicated plasmids and treated with the labeled anti-β1-integrin antibody as in (**A**) (upper). Images of Hoechst staining and labeled β1-integrin antibody, and the heat map images for the labeled β1-integrin antibody are shown. Bottom graphs indicate the intensity of labeled β1-integrin antibody signals along the arrows in the upper images.

chromatography on Probond™ Resin (Invitrogen). In preparation for the in vitro kinase assay, recombinant mouse vimentin was dialyzed with dialysis buffer (10 mM Tris-Cl, pH 8.8, 2 mM EGTA, 50 mM 2-mercaptoethanol, and 1 mM PMSF), and used within 1 wk.[16] For the phosphorylation assay of the early endosome fraction, purified His-tagged Plk1-WT or His-tagged Plk1-KD were mixed with the early endosome fraction, together with 50 μM ATP and 15 mM $MgCl_2$ in a final volume of 15 μl, and then incubated for 20 min at 30 °C in the presence of 3 μCi of [γ-^{32}P] ATP. For phosphorylation of mouse vimentin, purified His-tagged Plk1 proteins were mixed with mouse vimentin, together with 50 μM ATP and 1.5 mM $MgCl_2$, and incubated for 1 h at 25 °C. The reactions were stopped by the adding Leammli sample buffer and boiling.

Phosphoproteome analysis

The early endosome fraction from HeLa cells arrested in metaphase was dephosphorylated, mixed with recombinant His-tagged Plk1-WT or His-tagged Plk1-KD, and incubated at 30 °C for 20 min. The early endosome fractions were then digested with trypsin. A 100 μL aliquot of the peptide solution from the Plk1-WT or Plk1-KD treatment was mixed with 4 μL of 4% $^{13}CD_2O$ or $^{12}CH_2O$, respectively, and then 4 μL of freshly prepared 0.6 M sodium cyanoborohydride was immediately added. The mixture was agitated for 1 min and then incubated for 60 min at room temperature to achieve a labeling efficiency of more than 99%. The reaction was stopped by adding 16 μL of 1% ammonium hydroxide on ice and agitating the mixture for 1 min. The differentially labeled peptides were mixed and subjected to lactic acid-modified titania chromatography, as described.[21,22] For phosphoproteome analysis of synchronized cells, cell extracts were digested with trypsin and labeled with $^{13}CD_2O$ and $^{12}CH_2O$ for M phase-arrested cells and BI2539-treated, M phase-arrested cells or G_1/S phase-arrested cells, respectively, and then mixed. Phosphopeptide enrichment was done by titania. The differentially labeled peptides were mixed and the titania-based phosphopeptide enrichment was performed. NanoLC-MS/MS analyses were conducted with a TripleTOF 5600 mass spectrometer (ABSciex) equipped with aUltiMate 3000 RSLCnano pump (Thermo Fisher Scientific) and a HTC-PAL autosampler (CTC Analytics). Reprosil-Pur C18-AQ materials were packed into a self-pulled needle (150-mm length × 100 μm ID, 6-μm opening). The injection volume was 5 μL, and the flow rate was 500 nL/min. The mobile phases consisted of (A) 0.5% acetic acid and (B) 0.5% acetic acid in 80% acetonitrile. A 3-step linear gradient of 5–10% B in 5 min, 10–40% B in 60 min, and 40–100% B in 5 min, followed by 100% B for 10 min was employed. Spray voltages of 2300 V were applied. The mass scan ranges were *m/z* 300–1500, and the top 10 precursor ions were selected in each MS scan for subsequent MS/MS scans. Peptides and proteins were identified by Mascot v2.3 (Matrix Science) against UniProtKB/SwissProt with a precursor mass tolerance of 20 ppm, a fragment ion mass

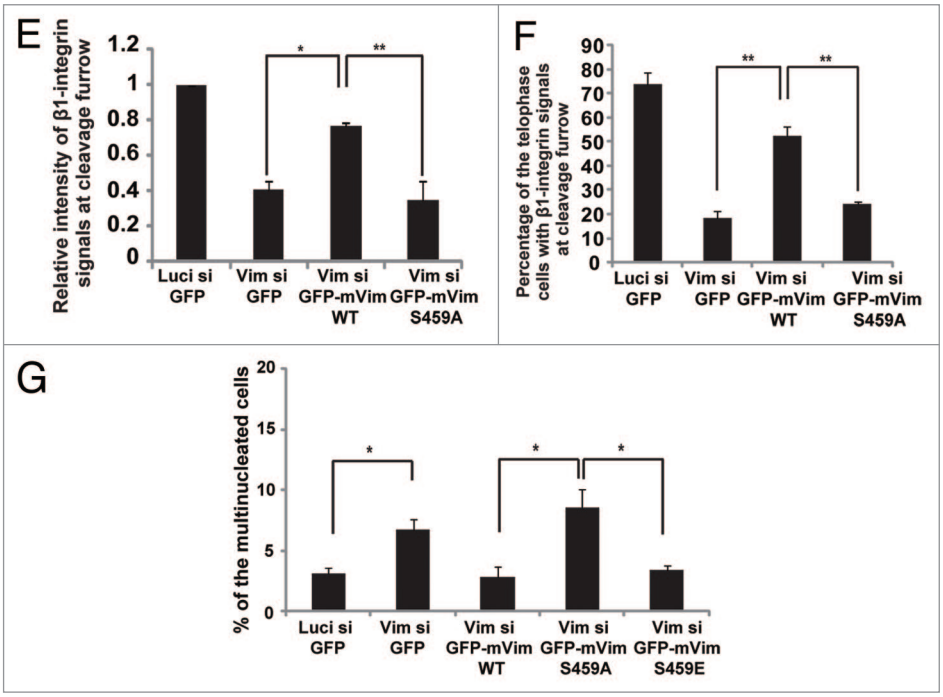

Figure 4E–G. (**E**) The relative intensity of labeled β1-integrin antibody signals at the cleavage furrow in the cells in (**D**) (mean ± s.e.m. from 3 different experiments; n = 12/experiment). *P < 0.05, **P < 0.01, analyzed by Dunnett multiple-comparison test. (**F**) The percentage of the cells with β1-integrin signals at the cleavage furrow (mean ± s.e.m. from 3 different experiments; n > 50/experiment). **P < 0.01, analyzed by Dunnett multiple-comparison test. The scale bar represents 5 μm. (**G**) The percentage of the multinucleated cells transfected with the indicated siRNAs together with the indicated plasmids and synchronized in G_1/S phase after released from a double-thymidine block (mean ± s.e.m. from 3 different experiments; n > 200/experiment). *P < 0.05, analyzed by *t* test in the left 2 columns and by Dunnett multiple-comparison test in the right 3 columns.

tolerance of 0.1 Da and strict trypsin specificity, allowing for up to 2 missed cleavages. Cysteine carbamidomethylation was set as a fixed modification, and methionine oxidation was allowed as a variable modification. Dimethylation of N-termini and ε-amino groups of lysine and phosphorylation of serine, threonine, and tyrosine were set as variable modifications. Peptide quantitation was performed using Mass Navigator (Mitsui Knowledge Industry), based on the integrated peak areas, and the heavy- and light-labeled peptide ratio (H/L ratio) was calculated for individual runs.

Cell staining and image analysis

For detecting EEA1 and CIMPR, cells were fixed with 3.7% formalin for 10 min in 37 °C and permeabilized with 0.2% Triton X-100 in PBS for 5 min. The cells were blocked with 3% BSA in PBS at 37 °C for 20 min, incubated with primary antibodies at 4 °C overnight, washed, and incubated for 1 h with secondary antibodies (AlexaFluor 488- or 546-conjugated goat anti-mouse IgG, Molecular Probes). For detecting β1-integrin, cells were incubated with anti-β1-integrin antibodies (P5D2) labeled with a ZenonAlexa Fluor 546 Mouse IgG Labeling kit (Molecular Probes) for 30 min at 37 °C, washed with DMEM, incubated for 30 min to allow the antibodies to be internalized into the cells and then fixed. For measuring the volume of EEA1 or CIMPR signals, the Z-stack images (0.3 μm apart) of cells were deconvoluted and converted to 3D images using Meta Morph software (Molecular Devices). For analyzing the relative intensity of β1-integrin signals, the single image with highest intensity of β1-integrin signals at the cleavage furrow was selected from the deconvoluted Z-stack images (0.3 μm apart), and the average intensity of the furrow region was measured. The heat map images were generated with ImageJ.

Time-lapse imaging of β1-integrin

HeLa cells were transfected with siRNAs by using Oligofectamine, incubated for 4 h, and subjected to a double-thymidine block. At the time of the secondary thymidine treatment, cells were trypsinized and plated onto 2-well coverglass chambers (IWAKI) coated with collagen, then incubated for 15 h to be synchronized in G_1/S phase. Ten hours after release from the double-thymidine block, cells were incubated with Alexa Fluor 546-labeled anti-β1-integrin antibodies (see above) for 30 min at 37 °C and washed with DMEM. During acquisition, cells were cultured in DMEM with 20 mM Hepes (pH 7.2). Time-lapse images were obtained with an Olympus IX81-ZDC microscope with a temperature-controlled, motorized stage, and were analyzed with Meta Morph software (Molecular Devices). Time-lapse images were taken every 40 s for 2 h.

Disclosure of Potential Conflicts of Interest

No potential conflicts of interest were disclosed.

Acknowledgments

We thank T Ohya for his technical expertise with early endosome fractionation. We thank J Hejna for editing and critical review of the manuscript. This work was supported by grants from the Funding Program for Next Generation World-leading Researchers (FT LS069), Grant-in-Aid for Young Scientists (A) (FT 21687017), and Grant-in-Aid for Scientific Research on Innovative Areas (FT 21113513).

Supplemental Materials

Supplemental materials may be found here:
www.landesbioscience.com/journals/cc/article/26866

References

1. GruenbergJ. The endocytic pathway: a mosaic of domains.Nat Rev Mol Cell Biol2001; 2:721-30; PMID:11584299; http://dx.doi.org/10.1038/35096054
2. ZerialM, McBrideH. Rab proteins as membrane organizers.Nat Rev Mol Cell Biol2001; 2:107-17; PMID:11252952; http://dx.doi.org/10.1038/35052055
3. TuomikoskiT, FelixMA, DoréeM, GruenbergJ. Inhibition of endocytic vesicle fusion in vitro by the cell-cycle control protein kinase cdc2.Nature1989; 342:942-5; PMID:2556645; http://dx.doi.org/10.1038/342942a0
4. FieldingAB, SchonteichE, MathesonJ, WilsonG, YuX, HicksonGR, SrivastavaS, BaldwinSA, PrekerisR, GouldGW. Rab11-FIP3 and FIP4 interact with Arf6 and the exocyst to control membrane traffic in cytokinesis.EMBO J2005; 24:3389-99; PMID:16148947; http://dx.doi.org/10.1038/sj.emboj.7600803
5. PellinenT, TuomiS, ArjonenA, WolfM, EdgrenH, MeyerH, GrosseR, KitzingT, RantalaJK, KallioniemiO, et al.Integrin trafficking regulated by Rab21 is necessary for cytokinesis.Dev Cell2008; 15:371-85; PMID:18804435; http://dx.doi.org/10.1016/j.devcel.2008.08.001
6. BastosRN, BarrFA. Plk1 negatively regulates Cep55 recruitment to the midbody to ensure orderly abscission.J Cell Biol2010; 191:751-60; PMID:21079244; http://dx.doi.org/10.1083/jcb.201008108
7. ChesneauL, DambournetD, MachicoaneM, KourantiI, FukudaM, GoudB, EchardA. An ARF6/Rab35 GTPase cascade for endocytic recycling and successful cytokinesis.CurrBiol2012; 22:147-53; PMID:22226746; http://dx.doi.org/10.1016/j.cub.2011.11.058
8. GorvelJP, ChavrierP, ZerialM, GruenbergJ. rab5 controls early endosome fusion in vitro.Cell1991; 64:915-25; PMID:1900457; http://dx.doi.org/10.1016/0092-8674(91)90316-Q
9. SimonsenA, LippéR, ChristoforidisS, GaullierJM, BrechA, CallaghanJ, TohBH, MurphyC, ZerialM, StenmarkH. EEA1 links PI(3)K function to Rab5 regulation of endosome fusion.Nature1998; 394:494-8; PMID:9697774; http://dx.doi.org/10.1038/28879
10. LanzettiL, MargariaV, MelanderF, VirgiliL, LeeMH, BartekJ, JensenS. Regulation of the Rab5 GTPase-activating protein RN-tre by the dual specificity phosphatase Cdc14A in human cells.J BiolChem2007; 282:15258-70; PMID:17371873; http://dx.doi.org/10.1074/jbc.M700914200
11. SchuPV, TakegawaK, FryMJ, StackJH, WaterfieldMD, EmrSD. Phosphatidylinositol 3-kinase encoded by yeast VPS34 gene essential for protein sorting.Science1993; 260:88-91; PMID:8385367; http://dx.doi.org/10.1126/science.8385367
12. FuruyaT, KimM, LipinskiM, LiJ, KimD, LuT, ShenY, RamehL, YanknerB, TsaiLH, et al.Negative regulation of Vps34 by Cdk mediated phosphorylation.Mol Cell2010; 38:500-11; PMID:20513426; http://dx.doi.org/10.1016/j.molcel.2010.05.009
13. LaneHA, NiggEA. Cell-cycle control: POLO-like kinases join the outer circle.Trends Cell Biol1997; 7:63-8; PMID:17708908; http://dx.doi.org/10.1016/S0962-8924(96)10051-9
14. ArchambaultV, GloverDM. Polo-like kinases: conservation and divergence in their functions and regulation.Nat Rev Mol Cell Biol2009; 10:265-75; PMID:19305416; http://dx.doi.org/10.1038/nrm2653
15. SütterlinC, LinCY, FengY, FerrisDK, EriksonRL, MalhotraV. Polo-like kinase is required for the fragmentation of pericentriolar Golgi stacks during mitosis.ProcNatlAcadSci U S A 2001; 98:9128-32; PMID:11447294; http://dx.doi.org/10.1073/pnas.161283998
16. YamaguchiT, GotoH, YokoyamaT, SilljéH, HanischA, UldschmidA, TakaiY, OguriT, NiggEA, InagakiM. Phosphorylation by Cdk1 induces Plk1-mediated vimentin phosphorylation during mitosis.J Cell Biol2005; 171:431-6; PMID:16260496; http://dx.doi.org/10.1083/jcb.200504091
17. MatsumuraS, ToyoshimaF, NishidaE. Polo-like kinase 1 facilitates chromosome alignment during prometaphase through BubR1.J BiolChem2007; 282:15217-27; PMID:17376779; http://dx.doi.org/10.1074/jbc.M611053200
18. RobertsRL, BarbieriMA, UllrichJ, StahlPD. Dynamics of rab5 activation in endocytosis and phagocytosis.J LeukocBiol2000; 68:627-32; PMID:11073100

19. WilsonDW, WilcoxCA, FlynnGC, ChenE, KuangWJ, HenzelWJ, BlockMR, UllrichA, RothmanJE. A fusion protein required for vesicle-mediated transport in both mammalian cells and yeast.Nature1989; 339:355-9; PMID:2657434; http://dx.doi.org/10.1038/339355a0
20. ClaryDO, GriffIC, RothmanJE. SNAPs, a family of NSF attachment proteins involved in intracellular membrane fusion in animals and yeast. Cell1990; 61:709-21; PMID:2111733; http://dx.doi.org/10.1016/0092-8674(90)90482-T
21. HsuJL, HuangSY, ChowNH, ChenSH. Stable-isotope dimethyl labeling for quantitative proteomics. Anal Chem2003; 75:6843-52; PMID:14670044; http://dx.doi.org/10.1021/ac0348625
22. SugiyamaN, MasudaT, ShinodaK, NakamuraA, TomitaM, IshihamaY. Phosphopeptide enrichment by aliphatic hydroxy acid-modified metal oxide chromatography for nano-LC-MS/MS in proteomics applications.Mol Cell Proteomics2007; 6:1103-9; PMID:17322306; http://dx.doi.org/10.1074/mcp.T600060-MCP200
23. DephoureN, ZhouC, VillénJ, BeausoleilSA, BakalarskiCE, ElledgeSJ, GygiSP. A quantitative atlas of mitotic phosphorylation.ProcNatlAcadSci U S A2008; 105:10762-7; PMID:18669648; http://dx.doi.org/10.1073/pnas.0805139105
24. RizkiA, MottJD, BissellMJ. Polo-like kinase 1 is involved in invasion through extracellular matrix. Cancer Res2007; 67:11106-10; PMID:18056432; http://dx.doi.org/10.1158/0008-5472.CAN-07-2348
25. IvaskaJ, VuoriluotoK, HuovinenT, IzawaI, InagakiM, ParkerPJ. PKCepsilon-mediated phosphorylation of vimentin controls integrin recycling and motility.EMBO J2005; 24:3834-45; PMID:16270034; http://dx.doi.org/10.1038/sj.emboj.7600847
26. BergelandT, HaugenL, LandsverkOJ, StenmarkH, BakkeO. Cell-cycle-dependent binding kinetics for the early endosomal tethering factor EEA1.EMBO Rep2008; 9:171-8; PMID:18188183; http://dx.doi.org/10.1038/sj.embor.7401152
27. GouldGW, Lippincott-SchwartzJ. New roles for endosomes: from vesicular carriers to multi-purpose platforms.Nat Rev Mol Cell Biol2009; 10:287-92; PMID:19277045; http://dx.doi.org/10.1038/nrm2652
28. FürthauerM, González-GaitánM. Endocytosis and mitosis: a two-way relationship.Cell Cycle2009; 8:3311-8; PMID:19770584; http://dx.doi.org/10.4161/cc.8.20.9700
29. TsuboiT, FukudaM. Rab3A and Rab27A cooperatively regulate the docking step of dense-core vesicle exocytosis in PC12 cells.J Cell Sci2006; 119:2196-203; PMID:16684812; http://dx.doi.org/10.1242/jcs.02962
30. IshidaM, OhbayashiN, MarutaY, EbataY, FukudaM. Functional involvement of Rab1A in microtubule-dependent anterograde melanosome transport in melanocytes.J Cell Sci2012; 125:5177-87; PMID:22854043; http://dx.doi.org/10.1242/jcs.109314